

Synthesis, Radiolabeling, and Biological Evaluation of Peptide LIKKPF Functionalized with HYNIC as Apoptosis Imaging Agent

Sepideh Khoshbakht^a, Davood Beiki^b, Parham Geramifar^b, Farzad Kobarfard^c, Omid Sabzevari^d, Mohsen Amini^e, Faramarz Mehrnejad^f and Soraya Shahhosseini^{g*}

^aDepartment of Radiopharmacy, Faculty of Pharmacy, Tehran University of Medical Sciences. ^bResearch Center for Nuclear Medicine, Tehran University of Medical Sciences. ^cDepartment of Pharmaceutical Chemistry, School of Pharmacy, Phytochemistry Research Center, Shahid Beheshti University of Medical Sciences. ^dDepartment of Toxicology and Pharmacology, Faculty of Pharmacy, and Toxicology and Poisoning Research Center, Tehran University of Medical Sciences. ^eDepartment of Medicinal Chemistry, and Drug Design and Development Research Center, Faculty of Pharmacy, Tehran University of Medical Sciences. ^fDepartment of Life Science Engineering, Faculty of New Sciences & Technologies, University of Tehran. ^gDepartment of Pharmaceutical Chemistry, School of Pharmacy, and PET/CT Unit, Ferdous Nuclear Medicine Center, Masih Daneshvari Hospital, Shahid Beheshti University of Medical Sciences, Tehran, Iran.

Abstract

A noninvasive method of detecting exposure of phosphatidylserine (PS) on the external surface of the plasma membrane such as nuclear imaging could assist the diagnosis and therapy of apoptosis related pathologies. The most studied imaging agent for apoptosis is Annexin V so far. Because of limitations of Annexin V other agents have been introduced such as small peptides and molecules. Radiopeptides that have affinity and bind to PS are good candidates for noninvasive imaging of apoptosis. The LIKKPF, introduced by Burtea *et al*, with nanomolar affinity for PS, was used as template. The biological properties of LIKKPF radiolabeled with Tc-99m was assessed *in-vitro* using apoptotic Jurkat cells and *in-vivo* using mouse model of liver apoptosis. The radiolabeled LIKKPF with ^{99m}Tc was stable in human serum at 37°C for at least 2 h. Results showed that the radiolabeled LIKKPF has less affinity to PS compare to original phage peptide, but high enough for specific binding to apoptotic cells *in-vitro* and *in-vivo*. It is concluded that the less affinity of radiolabeled LIKKPF might be attributed to hydrophobicity of peptide. The future peptides should be more hydrophobic compare to LIKKPF.

Keywords: Radiopeptide; Apoptosis; Phosphatidylserine; ¹⁸F-DG; ^{99m}Tc.

Introduction

Monitoring of apoptosis, the programmed cell death, in various pathology conditions

such as degenerative diseases, tumor treatment, and myocardial infarction would provide necessary information for medical team. One of the early biochemical changes of apoptotic cells is exposure of PS on the external surface of the plasma membrane (1-6). A noninvasive method of detecting this process such as nuclear imaging using radiopharmaceuticals could assist

* Corresponding author:

E-mail: s_shahoseini@sbm.ac.ir
soraya.shahhosseini@gmail.com

the diagnosis and therapy of apoptosis related pathologies, which is useful in preclinical and clinical studies in human. Radioligands that have affinity and bind to PS are good candidates for noninvasive imaging of apoptosis (7-9). Annexin V with high affinity for PS has been radiolabeled with ^{99m}Tc and ^{18}F in apoptosis imaging studies. Annexin V (35 kDa) is a natural intracellular human phospholipid binding protein which needs extracellular Ca^{2+} for binding to PS (approximately 2.5 mM Ca^{2+}). Its rapid clearance from body, short blood half life, and inability to deference between apoptosis and necrosis makes the optimal imaging of apoptotic cells difficult (10-11). Regarding high potential of peptides in diagnosis and therapy, radiopeptides with high affinity to PS independent of Ca^{2+} are appropriate candidates for apoptosis imaging.

In the last decade various groups have tried to introduce peptides with high affinity for PS through phage display technology (12-16). The results of research by Burtea *et al* in 2009 showed that peptide LIKKPF has high affinity for PS ($K_d = 2 \times 10^{-9}\text{M}$). The peptide was conjugated with DTPA, labeled with Gadolinium, and tested as MRI contrast agent with apoptotic Jurkat cells and animal model of liver apoptosis (16). Because of low sensitivity of imaging agent, the result was moderately successful.

Kapty *et al* radiolabeled LIKKPF with ^{18}F prosthetic group N-succinimidyl-4- ^{18}F fluorobenzoate (^{18}F SFB) and determined the affinity of radiolabeled peptide (17-18). The radiochemical purity (RCP) was low. In order to improve RCP, a cystein residue was added to LIKKPF and the thiol reactive N-[6-(4- ^{18}F fluorobenzylidene) aminoxyhexyl] maleimide (^{18}F FBAM) was used as a prosthetic group. Although the modification of LIKKPF to CLIKKPF and radiolabeling with ^{18}F FBAM increased RCP but cyctein residue resulted in lower affinity.

For routine clinical SPECT imaging, ^{99m}Tc is the radionuclide of choice. This is because it has good radiation physical characteristics (IT, 140 keV (90), 6h) and is available through an inexpensive $^{99}\text{Mo}/^{99m}\text{Tc}$ generator. Furthermore, it is well developed and has varied chemistry (19). The application of radiopeptides as apoptosis imaging agents in assessing the

therapeutic response of tumors to radio/chemo therapy, extent of damage after myocardial infarction, and neurodegenerative diseases has encouraged our research group for design and synthesis of new peptides. To reach the goal, the LIKKPF with nanomolar affinity to PS was chosen as a template. In this study, the biological activity of synthesized HYNIC-LIKKPF radiolabeled with ^{99m}Tc was evaluated. The affinity of radiolabeled LIKKPF with ^{99m}Tc was assessed *in-vitro* using camptothecin treated Jurkat cells and *in-vivo* using mouse model of liver apoptosis by intraperitoneal injection of lipopolysacharid (LPS). Moreover, the stability, labelling efficiency, RCP, and LogP of radiolabeled peptide were determined.

Experimental

For this study, the amino acids and resin were obtained from Bachem (Bubendorf, Switzerland). Coupling reagents, HOBt and DIC were purchased from Sigma-Aldrich (St. Luis, MO, USA). Succinimidyl-N-Boc-HYNIC were purchased from ABX advanced Biochemical compounds GmbH (Radeberg, Germany). FITC-conjugated Annexin V was from Biologend (San Diego, USA) and was used according to the manufacturer's instructions. Propidium iodide (PI), Camptothecin, and lipopolysacharide were purchased from Sigma-Aldrich. All of the chemicals, solvents and reagents were of analytical quality and used without further purification. Silica gel 60 F₂₅₄ pre-coated aluminium sheets from Merck were used for TLC. Using normal serum, $^{99m}\text{TcO}_4^-$ was eluted from a $^{99}\text{Mo}/^{99m}\text{Tc}$ generator (Pars-isotope, Tehran, Iran).

The distribution of radioactivity on TLC was determined using a TLC Scanner Mini-Scan, MS.1000. This was equipped with flow count B-FC-1000 and gamma detector MS3200, (Bioscan, Washington, USA). Mass-Spectra was recorded on LC-MS Triple Quad 6410 Agilent Technologies using series 1200 HPLC system (Tokyo, Japan) column: C-18, 250 × 4.6 mm, 5 μm, mobile phase: A:H₂O + 0.1% TFA, B: Acetonitrile, flow rate: 1 mL/min, 20 μL, total run time: 40 min. A NaI well counter (Triathler multilabel tester, Hidex, Finland) and a dose

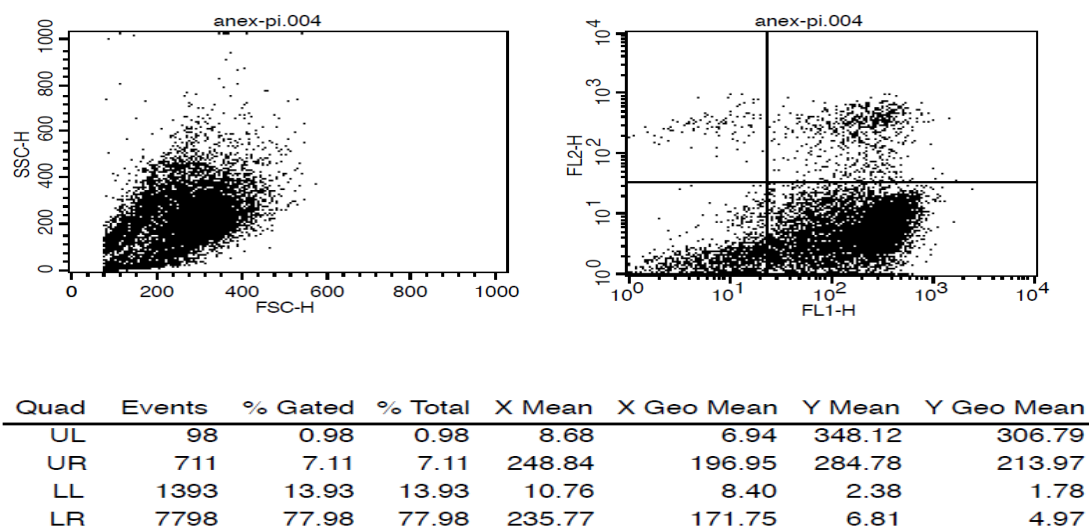


Figure 1. Flow cytometry of camptothecin treated Jurkat cells using Annexin V-FITC and PI.

calibrator (Atomlab 100, Biodex, NY) were used to measure low and high levels of radioactivity, respectively. Flow cytometric analysis were performed using a flow cytometer equipped with its accompanying software (FACSCalibur and CellQuestPro, respectively, Becton Dickinson).

Synthesis of peptide LIKKPF functionalized with HYNIC (HYNIC-LIKKPF)

Synthesis of peptide LIKKPF was done by using standard Fmoc strategy as described previously (20). Briefly, the peptide sequence Leu-Ile-Lye-Lye-Pro-Phe was assembled on Wang Resin with two equiv of N- α -Fmoc-protected amino acid (Phe) (Fmoc-Phe-OH) and two equiv HOBt and DIC as a coupling reagent in six steps. Removal of protecting group was carried out with 10% piperidine in DMF. Coupling of HYNIC to the last amino acid was done with 2 equiv of HATU, 3 equiv of DIPEA, two equiv of Succinimidyl-N-Boc-HYNIC in dry DMF. After shaking for 45 min at room temperature (RT), the solution was removed and the resin was washed with DMF and CH₂Cl₂, respectively. The completeness of the coupling reaction was checked by a Kaiser Test. The cleavage of peptide from resin was checked using cocktail TFA/TIS/H₂O (95:2.5:2.5) for 45 min (21). The solvents evaporated and peptide was precipitated with diethyl ether. The identity

of peptide was confirmed by LC-MS.

Stability of HYNIC-LIKKPF in serum

50 μ L of peptide (1 μ g/ μ L in ethanol) was added to 450 μ L of fresh human serum and incubated for 5, 10, 30, 60 and 120 min at 37°C. After incubation time, 500 μ L of acetonitrile was added to precipitate serum proteins. The mixture was centrifuged at 10000 g for 10 min. The supernatant was analyzed with LC-MS.

Labeling of HYNIC-LIKKPF with ^{99m}Tc

A detailed protocol of radiolabeling reaction of HYNIC-LIKKPF with ^{99m}Tc is available from the authors (20). The optimal condition of labelling: ^{99m}Tc-HYNIC-LIKKPF: RCP > 90%, (15-1000) μ g HYNIC-LIKKPF, 5 mg EDDA, 10 mg tricine, 7 μ g SnCl₂, pH 5-6, 100°C for 30 min.

Log P determination

Partition coefficient of radiolabeled peptide was determined in the mixture of PBS (pH 7.4) and n-octanol. 10 μ Ci of labeled peptide was added in 1 mL of PBS/n-octanol (1:1) mixture and vials were vortexed for 4 min and centrifuged at 5000 g for 10 min to separate two phases (aqueous and organic). 100 μ L of each phase was measured in a gamma counter. The Log P values were obtained in ratio of activity in organic phase to aqueous phase.

Table 1. Biological characteristics of radiolabeled peptide.

	Concentration	LogP	K _d	B _{max} nmol/cell
^{99m} Tc-HYNIC-LIKKPF	(20-100) nM	-0.87	(90 ± 21.06) nM	(1.141 × 10 ⁻¹³ ± 1.514 × 10 ⁻¹⁴)
LIKKPF		2.51*	2 nM *	

*calculated by Burtea *et al* (16).*Stability of radiolabeled peptide in serum*

The stability of ^{99m}Tc-HYNIC-LIKKPF was studied as previously reported (20). Briefly, 50 µCi of labeled peptide was added to 450 µL of fresh human serum and incubated at 37°C. At different time points plasma proteins were precipitated out by reacting with 0.5 mL acetonitrile. The mixture was centrifuged at 10000 g for 10 min. The activity bound to the plasma protein was measured by counting the activity associated with the precipitate. The supernatant was analysed by Radio-TLC [acetonitrile: water (95: 5)].

*In-vitro studies**Induction of apoptosis*

Human leukemia cells (Jurkat J6 cell, Pastur Institute, Tehran, Iran) were cultured in RPMI 1640 medium supplemented with 10% FBS, penicillin, and streptomycin. Apoptosis was induced on cells with camptothecin dissolved in DMSO to final concentration of 2 and 6 µM in growth medium and incubated in 5% CO₂ incubator at 37°C for 24 and 4 h respectively (22). Induction of apoptosis and percent of apoptotic cells were examined and measured by flow cytometry using Annexin V-FITC and PI. Camptothecin treated and untreated cells were harvested after 4 and 24 h, centrifuged for 5 min at 700 g, washed with cold PBS, and suspended in 1 mL cold binding buffer (HEPES 10 mM, NaCl 140 mM, BSA 1 mg/mL, CaCl₂ 2.5 mM, pH7.4). After addition of 5 µL (0.1 µg/µL) Annexin V-FITC and 15 min incubation at RT, 10 µL PI solution (1 µg/µL) was added and fluorescence intensity was measured using 2 color flow cytometry. Untreated cells and cells incubated with DMSO were considered as control.

Binding studies of radiolabeled peptide

A binding assay was performed in triplicate in the presence of increasing amounts of

radiolabeled peptide using apoptotic Jurkat cells. 500 µL of cell suspension in binding buffer was added to 1 mL Eppendorf tubes and incubated with increasing concentrations of radiolabeled peptide (2 × 10⁵ cells/mL, ^{99m}Tc-HYNIC-LIKKPF: S.A = 40 Ci/mmoL, 20 - 100 nM), for 30 min at room temperature. At the end of incubation times, the mixture was centrifuged (700 g, 5 min), the cell pellet was washed with cold binding buffer (3X) and the radioactivity of pellet was measured. Untreated cells used as negative control. For each radioligand concentration, nonspecific binding was determined by incubation of cells with excess amount of unlabeled peptide (100X of maximum concentration of radiolabeled peptide). The binding study was done in the presence and absence of calcium in binding buffer.

In-vivo studies

Balb/C adult mice (6-8 week old) were used and obtained from the breeding facility of the Department of Pharmacology and Toxicology, School of Pharmacy, Shahid Beheshti University of Medical Sciences. All animal studies were conducted in accordance with the guidelines established by the Shahid Beheshti University of Medical Sciences. Biodistribution studies were done in normal and apoptotic Balb/C mice (pre-treated and non-treated with cold peptide) with groups of 3 mice per each time point. Liver apoptosis was induced by intraperitoneal injection (IP) of lipopolysaccharid (LPS, Escherichia Coli, Serotype 055: B5, Sigma) dissolved in normal saline at a dose of 0.5 mg/Kg, 12 h before experiments (23). Pre-treated mice were received 200 µg cold peptide 30 min before injection of radiolabeled peptide.

Biodistribution studies of ^{99m}Tc-HYNIC-LIKKPF

One Hundred µCi of radiolabeled peptide (1 µCi/1 µL in saline) was injected via the

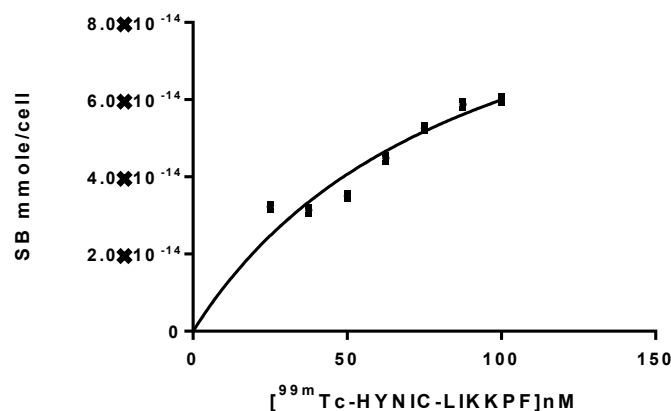


Figure 2. Saturation binding studies of ^{99m}Tc-HYNIC-LIKKPF, in camptothecin treated Jurkat cells.

tail vein of normal and apoptotic mice model, pre-treated and non-treated. The animals were sacrificed at 30 min, 2 h and 4 h post injection (n = 3 for each time point). Interested organs and tissues were separated, weighted, and counted. The results were reported as percentage of injected dose per gram of organ (%ID/g).

SPECT/CT imaging of normal and apoptotic mice

100 μ Ci of ^{99m}Tc-HYNIC-LIKKPF was injected via the tail vein of normal and apoptotic mice model. The mice were anesthetized intraperitoneally with ketamine HCl. Anesthesia was maintained by booster injections of ketamine. The SPECT/CT imaging was performed on the SIEMENS Symbia T clinical SPECT/CT scanner. The mice were placed in supine position and CT scans performed for anatomical reference and attenuation correction (spatial resolution 1.25 mm, 80 kV, 150 mAs) with a total CT scanning time of 10 sec. Dynamic SPECT images were acquired for 15 min (60 sec per frame) starting 30 sec after injection. The acquisition matrix size was 256 \times 256 and a zoom factor of 2.67 was used. The total counts of the liver, kidneys and bladder with related ratios were measured. SPECT/CT scans of healthy and liver apoptosis Balb/c mice were done 60 min after injection. The acquisition protocol was flash 3D with 256 \times 256 matrix size, 2.29 zoom factor and ninety 10-second views with both detectors. SPECT data were acquired with a noncircular orbit. Reconstruction was performed using the

flash 3D algorithm with 4 iterations and 20 subsets. Transmission data were reconstructed into a matrix of equal size by means of filtered back-projection, yielding a co-registered image set.

Results

We have already reported the synthesis and radiolabeling of HYNIC-LIKKPF with ^{99m}Tc (20).

The stability of HYNIC-LIKKPF was determined in serum. The peptide functionalized with HYNIC was incubated in fresh human serum (10X) at 37°C. After precipitation of serum proteins, the supernatant was analyzed with LC-MS. The results showed peptides were nearly 100% intact after 12 h.

The optimum conditions of radiolabeling of HYNIC-LIKKPF with ^{99m}Tc as previously reported is RCP > 90%, (15-1000) μ g peptide, 5 mg EDDA, 10 mg tricine, 7 μ g SnCl₂, 5-10 mCi ^{99m}Tc, pH 5-6, at 100°C for 30 min.

Log P of radiolabeled peptides was determined in PBS buffer and n-octanol. ^{99m}Tc-HYNIC-LIKKPF showed a Log P_{o/w} = -0.87.

Stability of radiolabeled peptide was checked in human fresh serum at 5, 10, 30, 60 and 120 min of incubation. The stability was analyzed by measuring the activity of precipitated serum proteins and TLC on supernatant. Results show that ^{99m}Tc radiolabeled peptide was 95% intact and only 5% of ^{99m}Tc released or transferred to serum proteins after 2 h.

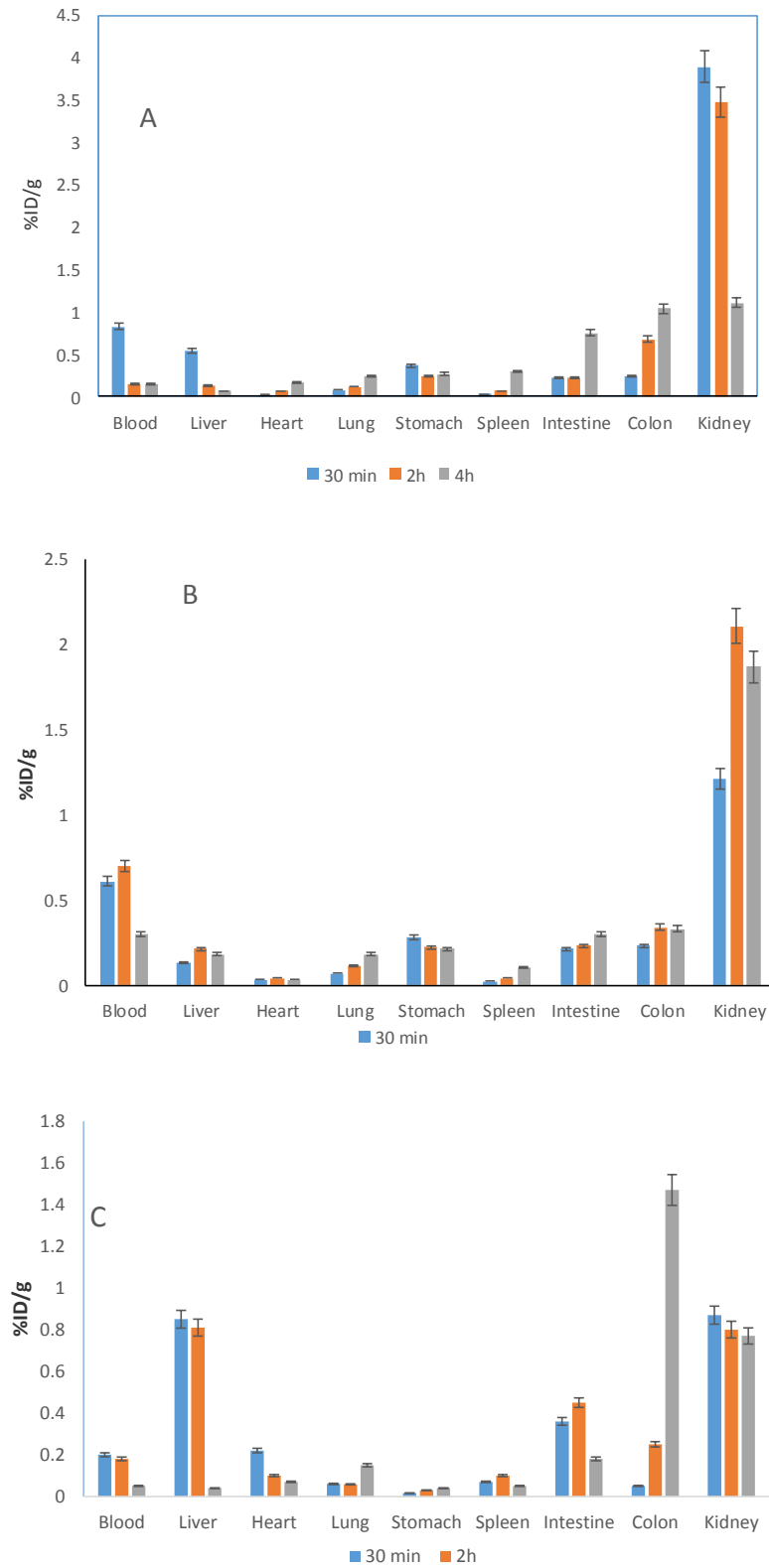


Figure 3. Biodistribution studies of ^{99m}Tc -HYNIC-LIKKPF in A) normal mice B) pre-treated mouse model of liver apoptosis C) non-treated mouse model of liver apoptosis at 30 min, 2 h, and 4 h post injection (n = 3). Radioactivity is shown in terms of % ID/g organ.

Apoptosis was induced in Jurkat cells by Camptothecin, a quinoline based DNA topoisomerase I inhibitor using two protocols (2 μ M, 24 h and 6 μ M, 4 h) (22). Results showed that apoptosis is achieved with both protocols. Apoptosis induction was confirmed by Flow cytometry using Annexin V-FITC and PI. There was less than 1% of cells dead, 78% apoptotic, 7% necrotic, and 14% unstain (Figure 1).

The affinity (K_d) of radiopeptide to PS was determined by saturation binding studies. Jurkat cells were incubated with increasing amount of radiolabeled peptides at RT. After incubation time, cell bound radiopeptide was separated from free by centrifuge. The specific binding (SB) was determined (Total bound-Non-specific bound, TB-NSB = SB). A plot of SB against concentration of radiopeptide was used for calculation of affinity (k_d) and B_{max} . The curve was fitted according to a sigmoidal dose response profile using Graph Pad Prism. Results are shown in Table 1 and Figure 2.

Biodistribution studies of radiolabeled LIKKPF was done in normal and mice model of liver apoptosis, pre-treated and non-treated. Mice were sacrificed at different time points, organs were separated, weighted, and activity measured. Results were reported as percentage of injected dose per gram of organs (%ID/g).

The distribution of radioactivity after IV injection of ^{99m}Tc -HYNIC-LIKKPF in normal and liver apoptosis mice is summarized as a function of time in Figure 3. The most prominent organs of uptake in normal mice include the kidneys, bladder, intestine, and colon. The remaining activity in the carcass and organs 30 min after injection was less than 15% of injected dose. It is apparent that the radioactivity rapidly cleared from blood and excreted in urine, suggesting renal clearance. Uptake in liver of apoptotic non-treated mice was 0.85% at 30 min (2.5 times normal values), 0.81% at 2 h (6.25 times normal values), which decreased to 0.05% at 4 h post injection. Kidney uptake was less than normal mice at all-time points. The renal activity decreased 22%, 23%, and 70% at 30 min, 2 and 4 h post injection, respectively. Colon uptake was 1.5 times above normal values 4 h post injection, suggesting hepatic clearance as well as kidney clearance. Hepatic uptake was inversely

proportional to renal uptake in apoptotic non-treated mice. The pattern of bio distribution of apoptotic mice pre-treated was similar to normal mice.

Generally speaking, accumulation of radio peptides in liver of apoptotic non-treated mice model was higher compare to normal and apoptotic pre-treated mice.

One Hundred μCi of ^{99m}Tc -HYNIC-LIKKPF was injected via the tail vein of normal and apoptotic mice model. As shown in Figure 4, the summation of the dynamic frames in the first 15 min clearly shows the significant activity concentration of tracer in kidneys, bladder and liver as it was seen in bio distribution studies as well. The liver to total frame counts were 7% and 9% for normal and liver apoptosis mouse model, respectively. For investigating the uptake behavior, the liver total counts were also measured in the SPECT/CT images of the mice acquired 60 min after injection. Based on mean count per number of pixels and data normalization of images, liver uptake has increased 63% compared to normal mouse.

Discussion

One of the early signs of apoptosis, within a few hours of apoptotic stimulus, is PS exposure on the extracellular face of the plasma membrane. PS is an abundant target. The most studied imaging agent for apoptosis is Annexin V and its fragments so far. Because of limitations of Annexin V (suboptimal pharmacokinetics, inability to distinguish apoptosis from necrosis, calcium dependent) other agents have been introduced such as small peptides and molecules (1-11). There is a need to develop a radioligand with better biodistribution profile for apoptosis imaging. Our group is currently working on design of new peptides as imaging agents for PS. The LIKKPF, introduced by Burtea *et al* with nanomolar affinity for PS, was selected as template. In this study, synthesis, conjugation, radiolabeling, and biological properties of radiolabeled LIKKPF was evaluated *in-vitro* and *in-vivo*.

Peptide LIKKPF was successfully synthesized via Fmoc strategy and functionalized with HYNIC at N-terminal. The structures were

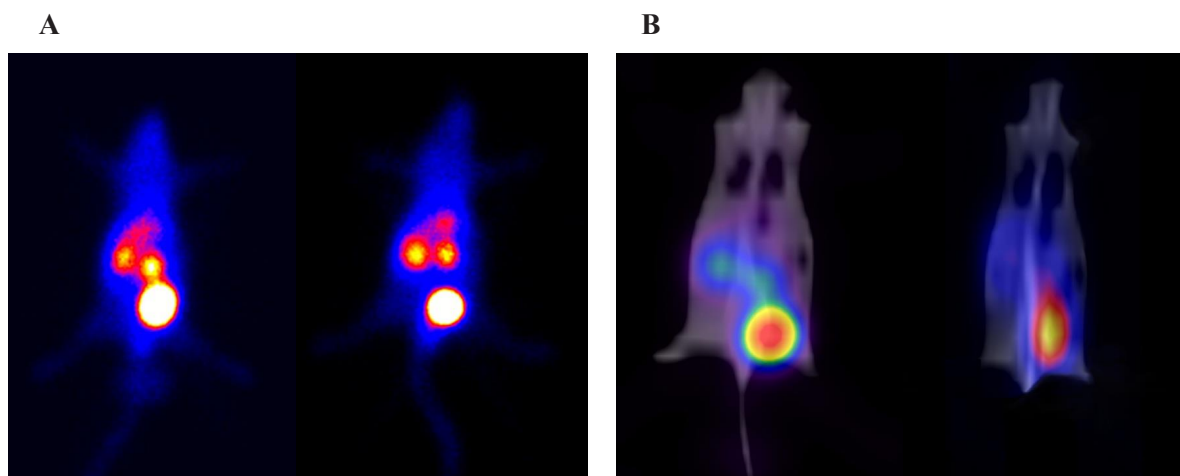


Figure 4. Balb/c mice after injection of 100 μCi $^{99\text{m}}\text{Tc}$ -HYNIC-LIKKPF. Mice were anesthetized with ketamine HCl. A) Summation of the first 15 min in a dynamic SPECT scan of healthy (left) and liver apoptosis (right). Tracer accumulation in the kidneys, bladder and liver were significant for both mice during the first 15 min after tracer injection. B) SPECT/CT fused image of healthy (left) and liver apoptosis (right) 60 min after injection.

confirmed with LC-MS. The functionalized peptide was stable in human serum at 37°C for at least 2 h. HYNIC conjugated LIKKPF was radiolabeled with $^{99\text{m}}\text{Tc}$ (RCP > 90%).

The radiolabeled LIKKPF was stable in human serum for at least 2 h at 37°C. LogP of radiolabeled LIKKPF was determined. The LogP value indicates high hydrophilicity of radiolabeled LIKKPF. The calculated LogP of LIKKPF by Burtea *et al* using ACDLabs 12.0 software was 2.51. Since each functional group of molecule contributes to the overall LogP, conjugation of HYNIC to LIKKPF and radiolabeling with $^{99\text{m}}\text{Tc}$ could be one of the reasons for significant reduction of LogP compare to original phage display LIKKPF. The reduced LogP of radiolabeled peptide explains its fast clearance from blood and excretion through kidneys.

The radiolabeled LIKKPF was tested *in-vitro* and *in-vivo*. The affinity of radiolabeled peptide was determined in saturation binding studies using camptothecine treated Jurkat cells. Results revealed that binding of radiolabeled LIKKPF to PS is not calcium dependent and radiolabeled peptide bind specifically to apoptotic cells. The level of binding to apoptotic cells was 2.5 times higher than control cells. The affinity of radiolabeled LIKKPF was lower than the original phage displayed peptide calculated by

Burtea *et al* (ELISA using phage, $K_d = 2.5$ nM). Kapy *et al* have also reported low affinity (18). There are two main reasons for low affinity of radiolabeled LIKKPF to PS. First, since more than 1 copy of peptide contribute in binding to target, the original phage displayed peptide has higher affinity with a better and more suitable conformation than single peptide (13). The second reason is low hydrophobicity of radiolabeled LIKKPF (negative LogP), which is responsible for peptide lipid interaction. Interaction of peptide with membrane lipid and polar PS head depends on its sequence. The positively charged residues (predominantly basic) provide electrostatic interactions with polar PS head group, while hydrophobic side chain residues hold peptide attached to membrane through hydrophobic interactions, which allows electrostatic interactions with the neighboring basic residues (3, 16). Electrostatic interactions of LIKKPF with PS is achieved by lysine residues that are ionized at physiological pH 7.4, which suggest their interaction with the polar head of PS as was mentioned by Burtea *et al* (16). Hydrophobic residues, leucine, isoleucine, proline and phenylalanine thought to be responsible for hydrophobic interaction.

The affinity of fluorescent tagged LIKKPF and CLIKKPF determined by Kapy *et al* was 0.69 μM and 1.9 μM , respectively. They argued

that addition of cysteine residue at N-terminus and fluorescent tag are responsible for low affinity of peptides (18).

Although the affinity of radiolabeled LIKKPF was less than original phage peptide, the level of binding to apoptotic cells was 2.5 times higher than control cells.

In this study, a mouse model of liver apoptosis was used for *in-vivo* experiments by injection of LPS intraperitoneally 12 h before experiment. Bio distribution studies showed higher liver uptake of radio peptide in apoptotic non-treated mouse model compare to normal and pre-treated mouse. The *in-vivo* imaging results were consistent with bio distribution studies. *In-vivo* imaging of normal and mouse model of liver apoptosis also showed a high concentration of radio peptide in liver of mouse model observed by SPECT/CT 60 min after injection. The percentage of whole body activity per organ determined by region of interest (ROI) image analysis correlated with the percentage of ID/g organ determined by bio distribution studies. The measurements show the high uptake of the liver in apoptotic mice model with 63% increase compare to normal mouse. There is negligible liver uptake in the healthy mouse (Figure 4).

In conclusion, electrostatic and hydrophobic interactions of peptide with membrane are necessary for PS binding (3, 13, 16). The peptide should be attached to membrane for electrostatic interactions with the neighboring residues. The more hydrophobic peptides should be considered in designing new peptides for PS binding.

Abbreviations

HYNIC: 6-Hydrazinonicotinamide,
TFA: trifluoroacetic acid, Tricine: N-[tris
(hydroxymethyl) methyl] glycine,
HOBT: n-hydroxy benzotriazole,
DIC: diisopropylcarbodiimide,
DIPEA: diisopropylethylamine, DMF:
dimethylformamide, TIS: triisobutylsilane, MEK:
methyl ethyl ketone, EDDA: ethylenediamine
diacetate, Fmoc: 9-fluorenylmethoxycarbonyl,
RCP: radiochemical purity.

Acknowledgment

This study was supported by funds from Iranian National Science Foundation (INSF).

References

- (1) Blankenberg FG, Tait J, Ohtsuki K and Strauss HW. Apoptosis: The important of nuclear medicine. Nuclear Medicine Communication 2000; 21: 241-250.
- (2) Blankenberg FG. *In-vivo* Detection of Apoptosis. J Nucl Med 2008; 49: 81S-95S.
- (3) Stace C L, Ktistakis NT. Phosphatidic acid- and phosphatidylserine-binding proteins. Biochimica et Biophysica Acta 2006; 1761: 913-926.
- (4) Schutters K, Reutelingsperger C. Phosphatidylserine targeting for diagnosis and treatment of human diseases. Apoptosis 2010; 15:1072-1082.
- (5) Guy M, Hickman JA. Apoptosis and cancer chemotherapy. Cell Tissue Res 2000; 301: 143-152
- (6) Carter N, Hail Jr BZ, Konopleva M and Andreeff M. Apoptosis effector mechanisms: A requiem performed in different keys. Apoptosis 2006; 11: 889-904.
- (7) Hanshaw RG and Smith BD. New reagents for phosphatidylserine recognition and detection of apoptosis. Bioorganic & Medicinal Chemistry 2005; 13: 5035-5042.
- (8) Blankenberg FG, Katsikis PD, Tait JF, Davis RE, Naumovsk L, Ohtsuki K, Kopiwoda S, Abrams MJ, Darkes M, Robbins RC, Maecker HT, and Strauss HW. *In-vivo* detection and imaging of phosphatidylserine expression during programmed cell death. Pro. Natl. Acad. Sci. USA 1998; 95: 6349-6354.
- (9) Zhao M, Li Zhixin, and Bugenhagen S. ^{99m}Tc-Labeled Duramycin as a Novel Phosphatidylethanolamine-Binding Molecular Probe. The Journal of Nuclear Medicine 2008; 49: 8.
- (10) Li X, Link JM, Stekhova S, Yagle JK, Smit C, Krohn KA, and Tait JF. Site-Specific Labeling of Annexin V with F-18 for Apoptosis Imaging. Bioconjugate Chemistry 2008; 19: 1684-1688.
- (11) Post AM, Katsikis PD, Tait JF, Geaghan SM, Strauss HW, Blankenberg FG. Imaging cell death with radiolabeled annexin V in an experimental model of rheumatoid arthritis. Journal of Nuclear Medicine 2002; 45: 36P.
- (12) Shao R, Xiong C, Wen X, Gelovani JG, and Li Chum. Targeting Phosphatidylserine on Apoptosis Cell with Phages and Peptides Selected from a Bacteriophage Display Library. Molecular Imaging 2007; 6: 417-426.
- (13) Laumonier C, Segers J, Laurent S, Michel A, Coppee F, Belayew A, Elst LV, Muller RN. A new peptidic vector for molecular imaging of apoptosis identified by phage display technology. Journal of Biomolecular Screen 2006; 11: 537-545.
- (14) Thapa N, Kim S, So IS, Lee BH, Kwon IC, Choi K, Kim IS. Discovery of phosphatidylserine-recognizing peptide and its utility in molecular imaging of tumor apoptosis. J Cell Mol Med 2008; 12 (5A): 1649-1660.
- (15) Hong HY, Choi JS, Kim YJ, *et al.* Detection of apoptosis in a rat model of focal cerebral ischemia using a homing peptide selected from *in-vivo* phage display. J Control Release 2008; 131: 167.
- (16) Burtea C, Laurent S, Lancelot E, Ballet S, Murariu O,

- Rousseaux O, Port M, Vander E, Corot L, and Muller R N. Peptidic Targeting of Phosphatidylserine for the MRI Detection of Apoptosis in Atherosclerotic Plaques. *Molecular Pharmaceutics* 2009; 6 (6): 1903-1919.
- (17) Kapy J, Kniess T, Wuest F, Mercer JR. Radiolabeling of phosphatidylserine-binding peptides with prosthetic groups N-[6-(4-[¹⁸F] fluorobenzylidene) aminoxyhexyl] maleimide (¹⁸F]FBAM) and N-succinimidyl-4-[¹⁸F] florobenzoate (¹⁸F]SFB). *Applied Radiation and Isotopes* 2011; 69: 1218-1225.
- (18) Kapy J, Banman S, Goping IS, and Mercer JR. Evaluation of Phosphatidylserine-Binding Peptides Targeting Apoptosis Cells. *Journal of Bimolecular Screening* 2012; 17(10): 1293-1310.
- (19) Schibli R, Schubiger PA (2002) Current use and future potential of organometallic radiopharmaceuticals. *European Journal of Nuclear Medicine*. 29: 1529-1542.
- (20) Khoshbakht S, Kobarfard F, Beiki D, Sabzevari O, Amini M, Mehrnejad F, Tabib K, Shahhosseini S. HYNIC a bifunctional prosthetic group for the labeling of peptides with ^{99m}Tc and ¹⁸FDG. *Journal of Radioanalytical and Nuclear Chemistry*. 2016; 307 (2): 1125-1134.
- (21) Dulery V, Renaudet O, Dumy P. Ethoxyethylidene protecting group prevents N-overacylation in aminoxy peptide synthesis. *Tetrahedron*. 2007; 63: 11952-11958.
- (22) Mukherjee A, Kothari K, Toth G, Szemenyei E, Sarma H D, Kornyei J, Venkatesh M. ^{99m}Tc-labeled annexin V fragments: a potential SPECT radiopharmaceutical for imaging cell death. *Nuclear Medicine and Biology*. 2006; 33:635-643.
- (23) Zhong J, Deaciuc I V, Burikhanov R, Villiers W J S de. Lipopolysaccharide-induced liver apoptosis is increased in interleukin-10 knockout mice. *Biochimica et Biophysica Acta* 2006; 1762: 468-477.

This article is available online at <http://www.ijpr.ir>
